J. Fluid Mech. (1975), *vol.* 71, *part* 1, *pp.* 65–88
Printed in Great Britain

Boundary-layer theory for blast waves

By K. B. KIM,† S. A. BERGER, M. M. KAMEL, V. P. KOROBEINIKOV AND A. K. OPPENHEIM
University of California, Berkeley

(Received 19 August 1974)

The necessity for developing a boundary-layer theory in the case of blast waves stems from the fact that inviscid flow solutions often yield physically unrealistic results. For example, in the classical problem of the so-called non-zero counter-pressure explosion, one obtains infinite temperature and zero density in the centre at all times even after the shock front deteriorates into a sound wave. In reality, this does not occur, as a consequence, primarily, of heat transfer that modifies the structure of the flow field around the centre without drastically affecting the outer region. It is profitable, therefore, to consider the blast wave as a flow field consisting of two regions: the outer, which retains the properties of the inviscid solution, and the inner, which is governed by flow equations including terms expressing the effects of heat transfer and, concomitantly, viscosity. The latter region thus plays the role of a boundary layer. Reported here is an analytical method developed for the study of such layers, based on the matched asymptotic expansion technique combined with patched solutions.

1. Introduction

Recent experimental studies of explosions revealed the importance of more realistic knowledge of the structure of blast waves than that hitherto available. This became of particular interest for the study of non-steady flow fields generated by exothermic chemical reactions, and especially by focused laser beams (Lee, Soloukhin & Oppenheim 1969; Bach, Knystautas & Lee 1969; Oppenheim & Soloukhin 1973), a technique nowadays in vogue as a consequence of the exciting possibility of attaining by such means appropriate conditions for controlled fusion (Brueckner 1973).

In the literature, such a flow field became known as the *non-zero counter-pressure* blast wave. Its inviscid properties are available, having been determined either by straightforward numerical computations of the Lagrangian equations of motion using the von Neumann–Richtmeyer artificial viscosity technique (e.g. Brode 1955), or by semi-analytical methods, such as that of Belotserkovskii's integral relations, used by Korobeinikov & Chushkin (1966). All these solutions have the drawback of the physically unrealistic feature of infinite temperature and zero density at the centre for all times, even after the shock front has decayed into a sound wave. At the same time, one observes in laboratory experiments

† Present address: Jet Propulsion Laboratory, Pasadena, California.

interesting phenomena occurring inside blast waves, such as spherical flame kernels generating shock fronts (Kamel & Oppenheim 1971) and developing triple-wave intersections (Lee *et al.* 1969). The principal question that arises then is whether the region of the flow field where these phenomena take place can be still treated as inviscid, and, in particular, whether the results of such elaborate studies as those of Korobeinikov & Chushkin (1966) could be used for their interpretation.

More specifically, of particular significance in this respect is, in essence, the question of what is the thickness, or radius, of the region where dissipative effects have a controlling influence. This is equivalent to the task of determining a boundary-layer thickness. The basic reason for the existence of a boundary layer is the requirement that appropriate flow boundary conditions be satisfied: namely, zero velocity at the wall due to the action of viscosity. In the case of blast waves, one has a similar requirement associated with the condition of zero temperature gradient at the centre, which is achieved as a consequence of heat-transfer effects.

In principle one could obtain, for a given case, a numerical solution of the set of blast-wave equations, including the terms expressing the effects of transport properties. However, this would be economically prohibitive, even with the use of modern computational techniques, as well as pointless, since, as the problem has been formulated above, it is more profitable to know the limits of available inviscid solutions than to seek a new solution for each particular case.

Thus the existence of a boundary layer is here postulated, i.e. a region around the centre whose structure is governed by transport processes, bounded by a virtually inviscid flow field. In order to determine salient features of this layer, in particular its effective radius, an analytical procedure has been developed, based on the matched asymptotic expansion technique combined with patched solutions for the two regions of flow. Treated in this manner are the cases of point, line and plane symmetrical flows of perfect gases with constant specific heats and constant Prandtl number corresponding to relatively high Reynolds numbers, while viscosity is assumed to be proportional to a given power of the absolute temperature, and the heat-transfer coefficient is expressed in terms of the Rosseland approximation expressing the effects of both conduction and radiation.

Our concern about the effects of transport processes on blast waves is, of course, by no means unique. Sedov (1959) included in his text a thorough analysis of the conditions leading to self-similarity for blast waves, for which the effects of heat conduction are included. Korobeinikov (1957) obtained an approximate solution to this problem for spherical explosions, by the use of a co-ordinate expansion of the self-similar equations of motion around the centre of symmetry. However, he was concerned with blast waves whose structure is affected by transport processes throughout their extent, as is the case when the Reynolds number is relatively low; and his analysis is, therefore, not related to the concept of a boundary layer. More recently, Sychev (1965) and Bowen & Feay (1970) obtained uniformly valid solutions, by means of the matched asymptotic expansion technique, for self-similar blast waves consisting of an outer inviscid region and an inner viscous and heat-conducting region. Sychev's solution also assumes that the viscosity and thermal conductivity are linearly proportional to temperature,

while that of Bowen & Feay is limited to cylindrical blast waves and constant transport properties. Sychev's solution is for small times (of the order of the molecular relaxation time), and demonstrates the manner in which the infinitely-high temperatures at the centre develop. On the other hand, our interest is in times after these high temperatures have developed, and in the manner in which diffusive effects cause their decay.

In our case, the problem is that of non-self-similar blast waves whose behaviour is governed by two matched sets of partial differential equations expressing the principles of conservation of mass, momentum and energy for the inner and outer regions, respectively. The behaviour of the outer region is described in terms of exponential fits to known solutions of inviscid blast waves. The equations governing the flow in the inner region are first simplified by the application of the principle of least degeneracy, then the solutions are expressed in the form of co-ordinate expansions. The task of analysing the inner region is thus reduced to the problem of solving a system of first-order ordinary differential equations, subject to proper matching conditions with the outer flow, and the boundary condition of zero flow velocity and zero temperature gradient at the centre.

2. Description of the physical model

As already indicated, the flow field, other than in the region close to the origin, is that of an inviscid non-zero counter-pressure blast wave. The initial conditions are given by the solution for the self-similar zero counter-pressure wave, that is, one bounded by a shock of infinite Mach number. Since the temperature at the centre is, therefore, initially infinite and can be expected to remain extremely high for long times (Sychev 1965; Bowen & Feay 1970), thermal conduction cannot be the sole heat-transfer mechanism, and, at least for an initial period of time, thermal radiation must be taken into account. In fact, as will be shown later, for most typical cases of interest, if one considers heat conduction only, the resulting temperatures near the centre are too high for this to be the sole heat transport mechanism.

A determination of the relative importance of conductive and radiative energy transport is in general difficult for arbitrary values of the photon mean free path. The situation is considerably simplified if the photon mean free paths are either much larger than the characteristic dimensions of the blast wave or much shorter, so that the Planck or Rosseland mean absorption coefficient approximations, respectively, are valid. The former of these cases is the optically-thin or transparent case, while the latter is the optically-thick or opaque case.

The relative importance of the two transfer mechanisms is most easily seen by forming the ratio of heat transfer by thermal conduction to heat transfer by radiation. For the diffusion or Rosseland approximation this ratio is given by (Thomas & Penner 1964)

$$\alpha_1 = 3k/(16\sigma T^3 \bar{l}_{L,Ro}),$$

while for the transparent case the ratio is

$$\alpha_2 \cong k(\nabla T)/(4\sigma T^4 L\bar{k}_{L,Pl}),$$

in terms of the thermal conductivity k, Stefan–Boltzman constant σ, absolute temperature T, Rosseland mean free path $\bar{l}_{L,Ro}$, characteristic length L, typical temperature gradient ∇T, and Planck mean absorption coefficient $\bar{k}_{L,Pl}$. The Rosseland approximation applies when $\bar{l}_{L,Ro} \ll L$; while for $\bar{l}_{L,Pl} (\equiv \bar{k}_{L,Pl}^{-1}) \gg L$ the transparent gas approximation is valid. However, since these parameters take no account of the motion of the fluid, only the first of these ratios is applicable to flow problems with radiant energy transport. Moreover, in the Rosseland limit the radiative and conductive heat-transfer coefficients are additive, while in the transparent limit, the more meaningful ratio is that of radiative energy loss from the system per unit surface area to a characteristic rate of enthalpy transport per unit area (Goulard 1964; Thomas & Penner 1964).

The most comprehensive tabulation of k, $\bar{l}_{L,Ro}$, $\bar{k}_{L,Pl}$ and the ratios α_1 and α_2 as functions of a broad range of densities and (high) temperatures is that of Thomas & Penner (1964). The work of Sychev (1965), Bowen & Feay (1970) and Brode (1968) for the case of nuclear blasts, and our solutions (anticipating the results) indicate that the temperatures and densities near the centre, for the cases of most interest, lie in a range of values for which, as indicated by Thomas & Penner (1964), we can conclude that $\bar{l}_{L,Ro}$ is much less than the characteristic length of the explosion,† and that $\alpha_1 \ll 1$. That is, the Rosseland approximation is valid in the very hot inner region. (In the outer region, the temperature is of the order of thousands of degrees and the air is transparent. The effects of either conduction or radiation are there relatively insignificant, and can be treated in the classical inviscid manner.) It is well known (Vincenti & Kruger 1965; Penner & Olfe 1968) that, in the Rosseland limit for an optically thick gas, the heat transfer by radiative transfer is proportional to the temperature gradient, so that the total heat conduction vector $\mathbf{q}$ can be written as the sum

$$\mathbf{q} = -(k + k_R)\nabla T.$$

k is the usual molecular thermal conduction coefficient; and k_R is a radiation conductivity given by

$$k_R = \tfrac{16}{3}\sigma T^3 \bar{l}_{L,Ro}.$$

(This result has already been used in forming the ratio α_1 above.)

Anticipating the importance of radiation, we shall represent the total effective conductivity χ $(= k + k_R)$, which in general is a function of both density and temperature, in such a manner that, by appropriate choice of certain parameters, the case of thermal conduction without radiation and that of radiation without conduction can be separately considered. In most cases, when radiation is considered, conduction is in fact negligible.

3. Conservation equations

The unsteady, one-dimensional flow field of a blast wave is described in terms of two independent variables, the time t and the space co-ordinate r, while the

† Such a characteristic length is defined later (equation (105)).

conservation equations of mass, momentum and energy, describing the flow, can be expressed most conveniently in the divergence form (Oppenheim *et al.* 1971)

$$\frac{\partial}{\partial t}(\rho r^j)+\frac{\partial}{\partial r}(u\rho r^j)=0, \tag{1}$$

$$\frac{\partial}{\partial t}(u\rho r^j)+\frac{\partial}{\partial r}\left[\left(u^2+\frac{p}{\rho}\right)\rho r^j\right]=\rho r^j\left(\frac{jp}{\rho r}+\Omega_1\right), \tag{2}$$

and

$$\frac{\partial}{\partial t}\left[\left(e+\frac{u^2}{2}\right)\rho r^j\right]+\frac{\partial}{\partial r}\left[\left(e+\frac{u^2}{2}+\frac{p}{\rho}\right)u\rho r^j\right]=\rho r^j\Omega_2, \tag{3}$$

where

$$j=\left\{\begin{matrix}0 \text{ for plane symmetry,}\\ 1 \text{ for line symmetry,}\\ 2 \text{ for point symmetry,}\end{matrix}\right\} \tag{4}$$

for density ρ, pressure p, flow velocity u, internal energy e, body or dissipative force acting on a unit mass Ω_1, and rate of energy deposited per unit mass of substance or the energy dissipation terms Ω_2.

For the case considered here, where only viscosity and heat-transfer effects are taken into account, Ω_1 and Ω_2 can be written in the form

$$\Omega_1\equiv\frac{4}{3}\frac{\mu}{\rho}\left[\frac{\partial^2 u}{\partial r^2}+\frac{j}{r}\left(\frac{\partial u}{\partial r}-\frac{u}{r}\right)\right]+\frac{4}{3}\frac{1}{\rho}\frac{\partial\mu}{\partial r}\left(\frac{\partial u}{\partial r}-\frac{j}{2}\frac{u}{r}\right), \tag{5}$$

$$\Omega_2\equiv\frac{1}{\rho}\left\{\tfrac{4}{3}\mu\left[u\frac{\partial^2 u}{\partial r^2}+\left(\frac{\partial u}{\partial r}\right)^2-\frac{j(j-1)}{2}\left(\frac{u}{r}\right)^2\right]+\frac{4}{3}\frac{\partial\mu}{\partial r}\left(u\frac{\partial u}{\partial r}-\frac{j}{2r}u^2\right)+\frac{\chi}{r^j}\frac{\partial}{\partial r}\left(r^j\frac{\partial T}{\partial r}\right)+\frac{\partial\chi}{\partial r}\frac{\partial T}{\partial r}\right\}. \tag{6}$$

T is the local temperature; and μ and χ are, respectively, the coefficients of viscosity and heat transfer. According to the arguments presented in § 2, the latter can be expressed in terms of the Rosseland approximation as

$$\mu\equiv\mu_0\left(\frac{T}{T_0}\right)^\alpha \quad\text{and}\quad \chi\equiv\chi_0\left(\frac{T}{T_0}\right)^\alpha\left(\frac{\rho}{\rho_0}\right)^\delta. \tag{7), (8}$$

α and δ are constants, while a subscript zero refers to a reference state. Equation (8) represents the total effective heat-transfer coefficient, which by appropriate choice of α and δ allows us to take into account at the same time the effects of thermal conductivity and radiation.

The medium is assumed to behave essentially as a perfect gas with constant specific heats; and the conservation equations are expressed in non-dimensional form by the introduction of geometric blast-wave co-ordinates

$$x\equiv r/r_n \quad\text{and}\quad \xi=r_n/r_0,$$

and fluid flow parameters

$$f\equiv\frac{u}{W_n},\quad h\equiv\frac{\rho}{\rho_a},\quad g\equiv\frac{p}{\rho_a W_n^2},\quad y\equiv\left(\frac{a_a}{W_n}\right)^2=\frac{1}{M^2},\quad \lambda\equiv\frac{d\ln y}{d\ln\xi},$$

$$R\equiv\frac{r_0 a_a\rho_a}{\mu_0},\quad P\equiv\frac{\mu_0 c_p}{\chi_0}. \tag{9}$$

r_n is the front radius, r_0 its reference value, W_n its velocity and M its Mach number; a is the local speed of sound, c_p the specific heat at constant pressure; and a subscript a refers to the state of the ambient atmosphere, into which the blast wave propagates.

As a consequence of the perfect gas assumption,

$$T/T_a = \gamma g/(hy). \tag{10}$$

In terms of these non-dimensional quantities, (1)–(3), with (5) and (6), become

$$\frac{\partial \ln h}{\partial \ln \xi} - \left(1 - \frac{f}{x}\right)\frac{\partial \ln h}{\partial \ln x} + \frac{f}{x}\left(\frac{\partial \ln f}{\partial \ln x} + j\right) = 0, \tag{11}$$

$$-\frac{\lambda}{2} + \frac{\partial \ln f}{\partial \ln \xi} - \left(1 - \frac{f}{x}\right)\frac{\partial \ln f}{\partial \ln x} + \frac{g}{hfx}\frac{\partial \ln g}{\partial \ln x} = \omega_1, \tag{12}$$

$$-\lambda + \frac{\partial \ln g}{\partial \ln \xi} - \left(1 - \frac{f}{x}\right)\frac{\partial \ln g}{\partial \ln x} - \gamma\left[\frac{\partial \ln h}{\partial \ln \xi} - \left(1 - \frac{f}{x}\right)\frac{\partial \ln h}{\partial \ln x}\right] = \omega_2, \tag{13}$$

where

$$\omega_1 = \tfrac{4}{3}\gamma^\alpha \frac{M^{2\alpha-1}}{R\xi}\frac{g^\alpha}{fh^{\alpha+1}}\left[\frac{\partial^2 f}{\partial x^2} + \frac{j}{x}\frac{\partial f}{\partial x} - j\left(\frac{f}{x}\right)^2 + \alpha\left(\frac{1}{g}\frac{\partial g}{\partial x} - \frac{1}{h}\frac{\partial h}{\partial x}\right)\left(\frac{\partial f}{\partial x} - \frac{jf}{2x}\right)\right], \tag{14}$$

$$\begin{aligned}\omega_2 = \gamma^{\alpha+1}\frac{M^{2\alpha-1}}{RP\xi}\frac{1}{h^{1-\delta}g}\left(\frac{g}{h}\right)^\alpha \Bigg[& -\frac{g}{h}\frac{\partial^2 h}{\partial x^2} + \frac{\partial^2 g}{\partial x^2} - \frac{(2\alpha - \delta + 2)}{h}\frac{\partial h}{\partial x}\frac{\partial g}{\partial x} - \frac{jg}{xh}\frac{\partial h}{\partial x} \\ & + \frac{j}{x}\frac{\partial g}{\partial x} + (2 + \alpha - \delta)\frac{g}{h^2}\left(\frac{\partial h}{\partial x}\right)^2 + \frac{\alpha}{g}\left(\frac{\partial g}{\partial x}\right)^2\Bigg] \\ & + \frac{(\gamma - 1)}{g}\tfrac{4}{3}\gamma^\alpha \frac{M^{2\alpha-1}}{R\xi}\left(\frac{g}{h}\right)^\alpha\left[\left(\frac{\partial f}{\partial x}\right)^2 - \frac{jf}{x}\frac{\partial f}{\partial x} - \frac{j(j-3)}{2}\frac{f^2}{x^2}\right].\end{aligned} \tag{15}$$

γ is the specific heat ratio.

As indicated in § 1, (11)–(13) are solved by introducing the concept of a boundary-layer-like region, i.e. a region around the centre where the influence of transport processes is predominant, while outside this region such effects are negligible. The extent of the inner region is defined in terms of its radius $\tilde{r}$, the principal unknown of our problem.

4. Scaling

The flow field in the inner region, containing the dissipative effects, is described by a set of second-order nonlinear partial differential equations, which are not amenable to straightforward solution. In order to simplify these equations, an order-of-magnitude analysis is therefore required.

For this purpose, the equations are scaled by introducing the small parameter

$$\epsilon \equiv \tfrac{4}{3}(RP)^{-1}. \tag{16}$$

In terms of this parameter, the inner variables are scaled as

$$x_i \equiv x/\nu(\epsilon), \quad f_i \equiv f/\phi(\epsilon), \quad h_i \equiv h/\beta(\epsilon). \tag{17)–(19}$$

ν, ϕ and β are, at this stage, arbitrary functions of ϵ. We do not rescale g (i.e. the pressure) in the inner region. The reason for this is that the pressure of the

inviscid outer flow field is practically uniform around the centre; hence it is assumed to be simply impressed, without any distortion, upon the inner region.†

The second independent variable, ξ, is also not scaled since, as a measure of the shock front position, it describes the extent of the whole flow field at a given instant of time, and is therefore universally applicable to both the inner and outer regions.

The conservation equations for the inner region (11)–(13) become

$$\frac{\partial \ln h_i}{\partial \ln \xi} - \left(1 - \frac{\phi}{\nu}\frac{f_i}{x_i}\right)\frac{\partial \ln h_i}{\partial \ln x_i} + \frac{\phi}{\nu}\frac{f_i}{x_i}\left(\frac{\partial \ln f_i}{\partial \ln x_i} + j\right) = 0, \tag{20}$$

$$-\frac{\lambda}{2} + \frac{\partial \ln f_i}{\partial \ln \xi} - \left(1 - \frac{\phi}{\nu}\frac{f_i}{x_i}\right)\frac{\partial \ln f_i}{\partial \ln x_i} + \frac{1}{\nu\phi\beta}\frac{g}{h_i f_i x_i}\frac{\partial \ln g}{\partial \ln x_i}$$
$$= \frac{\epsilon P}{\nu^2 \beta^{\alpha+1}}\gamma^\alpha \frac{M^{2\alpha-1}}{\xi}\frac{g^\alpha}{f_i h_i^{\alpha+1}}\left[\frac{\partial^2 f_i}{\partial x_i^2} + \frac{j}{x_i}\frac{\partial f_i}{\partial x_i} - j\left(\frac{f_i}{x_i}\right)^2 + \alpha\left(\frac{1}{g}\frac{\partial g}{\partial x_i} - \frac{1}{h_i}\frac{\partial h_i}{\partial x_i}\right)\left(\frac{\partial f_i}{\partial x_i} - \frac{j}{2}\frac{f_i}{x_i}\right)\right], \tag{21}$$

and
$$-\lambda + \frac{\partial \ln g}{\partial \ln \xi} - \left(1 - \frac{\phi}{\nu}\frac{f_i}{x_i}\right)\frac{\partial \ln g}{\partial \ln x_i} - \gamma\left[\frac{\partial \ln h_i}{\partial \ln \xi} - \left(1 - \frac{\phi}{\nu}\frac{f_i}{x_i}\right)\frac{\partial \ln h_i}{\partial \ln x_i}\right]$$
$$= \frac{\epsilon}{\beta^{\alpha-\delta+1}\nu^2}\tfrac{3}{4}\gamma^{\alpha+1}\frac{M^{2\alpha-1}}{\xi}\frac{1}{h_i g}\frac{g^\alpha}{h_i^{\alpha-\delta}}\left[-\frac{g}{h_i}\frac{\partial^2 h_i}{\partial x_i^2} + \frac{\partial^2 g}{\partial x_i^2} + \frac{j}{x_i}\frac{\partial g}{\partial x_i}\right.$$
$$\left. - \frac{(2\alpha - \delta + 2)}{h_i}\frac{\partial h_i}{\partial x_i}\frac{\partial g}{\partial x_i} - \frac{jg}{x_i h_i}\frac{\partial h_i}{\partial x_i} + (2 + \alpha - \delta)\frac{g}{h_i^2}\left(\frac{\partial h_i}{\partial x_i}\right)^2 + \frac{\alpha}{g}\left(\frac{\partial g}{\partial x_i}\right)^2\right]$$
$$+ \frac{\epsilon P}{\beta^\alpha}\frac{\phi^2}{\nu^2}\frac{(\gamma - 1)}{g}\gamma^\alpha \frac{M^{2\alpha-1}}{\xi}\left(\frac{g}{h_i}\right)^\alpha\left[\left(\frac{\partial f_i}{\partial x_i}\right)^2 - \frac{j f_i}{x_i}\frac{\partial f_i}{\partial x_i} - \frac{j(j-3)}{2}\left(\frac{f_i}{x_i}\right)^2\right]. \tag{22}$$

Requiring that all the terms in the continuity equation be of the same order leads to

$$\nu(\epsilon) = \phi(\epsilon). \tag{23}$$

Now, applying the principle of least degeneracy (Van Dyke 1964), one finds that the heat-transfer term in the energy equation (22) should be of the same order of magnitude as the inviscid terms. This requires that

$$\beta^{\alpha+1-\delta}(\epsilon)\,\nu^2(\epsilon) = \epsilon. \tag{24}$$

This provides us with two relations for ν, ϕ and β in terms of ϵ. The third is obtained from the asymptotic inviscid solution at the centre, i.e. the inner limit of the outer solution. For instance, in the classical case of the constant energy, non-zero counter-pressure blast wave, it is known (see e.g. Korobeinikov & Chushkin 1966) that h can be expressed in the form

$$h \sim x^{(j+1)/(\gamma-1)}. \tag{25}$$

Then the zeroth-order inner solution, i.e. the part independent of ϵ, should be expressed asymptotically, for proper matching, as

$$h_i \sim \beta^{-1}(\nu x_i)^{(j+1)/(\gamma-1)}. \tag{26}$$

† In fact, we need not assume this to be the case. The validity of this assumption would follow automatically from the scaling (Sychev 1965; Bowen & Feay 1970).

	$\delta = 0$			$\delta = -2$
j	$\alpha = \frac{1}{6}$	$\alpha = 1$	$\alpha = -\frac{1}{2}$	$\alpha = 1{\cdot}5$
0	$\frac{1}{4{\cdot}9}$	$\frac{1}{7}$	$\frac{1}{3{\cdot}25}$	$\frac{1}{3{\cdot}25}$
1	$\frac{1}{7{\cdot}83}$	$\frac{1}{12}$	$\frac{1}{4{\cdot}5}$	$\frac{1}{4{\cdot}5}$
2	$\frac{1}{10{\cdot}75}$	$\frac{1}{17}$	$\frac{1}{5{\cdot}75}$	$\frac{1}{5{\cdot}75}$

TABLE 1. Value of the exponent ω of ϵ in $\nu(\epsilon) = \epsilon^{(\gamma-1)/[(j+1)(\alpha-\delta)+2\gamma+(j-1)]}$

From the condition that h_i be independent of ϵ, it follows that

$$\beta = \nu^{(j+1)/(\gamma-1)}. \tag{27}$$

This expression, combined with (23) and (24), yields finally

$$\nu(\epsilon) = \phi(\epsilon) = \epsilon^{(\gamma-1)/[(j+1)(\alpha-\delta)+2\gamma+(j-1)]}, \tag{28}$$

and

$$\beta(\epsilon) = \epsilon^{(j+1)/[(j+1)(\alpha-\delta)+2\gamma+(j-1)]}. \tag{29}$$

The function $\nu(\epsilon)$, given by (28), determines the size of the inner region. Table 1 gives a list, for various values of j, α and δ ($\gamma = 1{\cdot}4$), of the exponent ω of ϵ in the expression for $\nu(\epsilon)$. (As will be discussed in § 11, $\delta = 0$ corresponds to the thermal conduction case, and $\delta = -2$ to the radiation case. The significance of the particular choices of α will also appear later.) We take particular note of the generally small values of the exponent.

For $\epsilon \ll 1$, we note that the above relations lead to the inequalities or estimates

$$\nu\phi\beta \ll 1 \quad \text{and} \quad \epsilon/\beta^{\alpha} \ll 1, \tag{30), (31}$$

to be used in obtaining the equations for the inner region.

5. Governing equations

Using the results of § 4, the conservation equations for the inner region, (20)–(22), can be reduced as shown below. By virtue of the definition in (9),

$$\frac{\partial}{\partial \ln \xi} \equiv \lambda \frac{\partial}{\partial \ln y}; \tag{32}$$

and, in accordance with (23), the continuity equation (20) becomes

$$\lambda \frac{\partial \ln h}{\partial \ln y} - \left(1 - \frac{f}{x}\right) \frac{\partial \ln h}{\partial \ln x} + \frac{f}{x}\left(\frac{\partial \ln f}{\partial \ln x} + j\right) = 0. \tag{33}$$

As a consequence of the first reduction rule (30), the momentum equation (21) is reduced to the condition

$$\partial g/\partial x = 0, \quad \text{so that} \quad g = g(y), \tag{34}$$

which means that the pressure of the inviscid outer flow region, a plateau around the centre, is impressed uniformly upon the inner boundary layer throughout its extent. As the result of the second reduction rule (31), all the viscous terms in the energy equation vanish, and (22) becomes

$$-\lambda+\lambda\frac{\partial \ln g}{\partial \ln y}-\gamma\left[\lambda\frac{\partial \ln h}{\partial \ln y}-\left(1-\frac{f}{x}\right)\frac{\partial \ln h}{\partial \ln x}\right]$$
$$=-\frac{\gamma^{\alpha+1}y^{\frac{1}{2}-\alpha}}{RP}\frac{g^{\alpha}}{\xi}\frac{}{h^{2+\alpha-\delta}}\left[\frac{\partial^2 h}{\partial x^2}+\frac{j}{x}\frac{\partial h}{\partial x}-\frac{(2+\alpha-\delta)}{h}\left(\frac{\partial h}{\partial x}\right)^2\right]. \tag{35}$$

(Since viscous effects are in fact negligible in the inner region, the Reynolds number is not a very meaningful quantity, and the small parameter $\epsilon \equiv \frac{4}{3}(RP)^{-1}$ is simply the ratio of heat transfer by conduction or radiation to convective transfer.)

6. Boundary and matching conditions

Boundary conditions for the inner region are (i) symmetry conditions at the centre, to be satisfied at all times (i.e. for $\xi > 0$), namely, (*a*) zero particle velocity

$$f = 0 \quad \text{at} \quad x = 0, \tag{36}$$

(*b*) zero temperature gradient, which, as a consequence of the perfect gas assumption and (31), stipulates

$$\partial h/\partial x = 0 \quad \text{at} \quad x = 0; \tag{37}$$

(ii) matching conditions between the inner and outer regions

$$f_{\text{inner}} = f_{\text{outer}} \quad \text{at some} \quad x = \tilde{x}, \tag{38}$$

$$h_{\text{inner}} = h_{\text{outer}} \quad \text{at some} \quad x = \tilde{x}. \tag{39}$$

Here the derivatives are not matched, so that profiles of gasdynamic parameters for the two regions intersect each other at finite angles at the matching point. One of the virtues of this procedure, apart from its simplicity, is that it leads to a sharp criterion for the evaluation of $\tilde{x}$.

For the special case of a constant-energy blast wave with non-zero counter-pressure, the asymptotic inner limits of the outer inviscid flow field have the form (Korobeinikov & Chushkin 1966)

$$f_{\text{outer}} = F(y)\,x, \quad h_{\text{outer}} = H(y)\,x^s. \tag{40), (41}$$

Here, as a consequence of the conservation equations (11)–(13) (with $\omega_1 \equiv \omega_2 \equiv 0$) and the transformation (32),

$$F(y) = \frac{\lambda(y)}{\gamma(j+1)}\left\{1-\frac{d \ln g(y)}{d \ln y}\right\}, \tag{42}$$

$$H(y) = k_1 \exp\left\{\int_0^y \left[\frac{1}{\gamma-1}\left(\frac{j+1}{\lambda}-1\right)\frac{1}{y}+\frac{d}{dy}\frac{1}{g}\right]dy\right\}, \tag{43}$$

with

$$s = (j+1)/(\gamma-1). \tag{44}$$

The constant k_1, which appears in expression (43) for $H(y)$, is given, for $j = 2$, by

$$k_1 = \frac{(\gamma+1)^{[3\gamma(\gamma+1)]/(\gamma-1)(3\gamma-1)}}{2^{6/[5(\gamma-1)]}(\gamma-1)\gamma^{(7\gamma-1)/(\gamma-1)(3\gamma-1)}}\left(\frac{2\gamma+1}{7-\gamma}\right)^{(13\gamma^2-7\gamma+12)/[5(\gamma-1)(2-\gamma)(3\gamma-1)]}; \quad (45)$$

for $j = 1$, by

$$k_1 = \frac{(\gamma+1)^{(\gamma+1)/(\gamma-1)}}{(\gamma-1)}\frac{\gamma^{(3\gamma-4)/(\gamma-1)(2-\gamma)}}{2^{2/(\gamma-1)(2-\gamma)}}; \quad (46)$$

and for $j = 0$, by

$$k_1 = \frac{(2\gamma-1)^{(5\gamma-4)/[3(\gamma-1)(2-\gamma)]}(\gamma+1)^{(4+\gamma-3\gamma^2)/[3(\gamma-1)(2-\gamma)]}}{2^{2/[3(\gamma-1)]}\gamma^{1/(\gamma-1)}(\gamma-1)}. \quad (47)$$

The functions $\lambda(y)$ and $g(y)$, as well as $\xi(y)$, are given in numerical form by the inviscid flow solutions. For present purposes, they are approximated by the algebraic expressions

$$\lambda(y) = \lambda_0 + \lambda_1 y + \lambda_2 y^2 + \lambda_3 y^3 + \lambda_4 y^4, \quad (48)$$

$$g(y) = g_0 + g_1 y + g_2 y^2 + g_3 y^3 + g_4 y^4, \quad (49)$$

$$\xi(y) = [\xi_1 y \exp\{\xi_2 y \exp(\xi_3 y + \xi_4 y^2 + \xi_5 y^3 + \xi_6 y^4 + \xi_7 y^5 + \xi_8 y^6 + \xi_9 y^7)\}]^{1/(j+1)}. \quad (50)$$

Here (Bach & Lee 1970)

$$\xi_1 = \left(\frac{j+3}{2}\right)^2\gamma, \quad \xi_2 = \frac{-\lambda_1}{\lambda_0} \quad \text{and} \quad \lambda_0 = j+1. \quad (51), (52)$$

7. Initial conditions

Initial conditions are provided by the solution of the self-similar case, for which $y = 0$. Special attention must be paid to the factor $y^{\frac{1}{2}-\alpha}/\xi$, which appears on the right-hand side of (35). From (50) it follows that, for small y,

$$\frac{y^{\frac{1}{2}-\alpha}}{\xi} = (\xi_1^{-1})^{(j+1)^{-1}} y^{\frac{1}{2}-\alpha-(j+1)^{-1}} \quad (y \ll 1). \quad (53)$$

In order that the governing equations be independent of y, so that the flow, in a continuous manner, approaches the self-similar case with respect to x in the limit $y \to 0$, the exponent of y in (53) must vanish. Hence, for $\xi > 0$,

$$\alpha = \alpha_s = \tfrac{1}{2}(j-1)/(j+1). \quad (54)$$

If $\alpha > \alpha_s$, the right-hand side of (35) becomes infinite. This means that, under such circumstances, the whole flow field is so strongly influenced by heat transfer that the temperature gradient, and hence the density gradient, everywhere must be vanishingly small. In this case, the density at the centre is of the order of 1. On the other hand, if $\alpha < \alpha_s$, the left-hand side of (35) acquires a dominant role, so that the whole flow field is, in effect, inviscid, and the temperature at the centre is infinite while the density is zero. Neither of these extreme cases provides proper initial conditions for a heat-conducting boundary layer. Thus, for $\alpha \neq \alpha_s$, another procedure is required.

8. Co-ordinate transformation

To remedy the situation described at the end of § 7 (i.e. to determine proper initial conditions for the case when $\alpha \neq \alpha_s$), following Sychev (1965) we substitute for the geometric space co-ordinate x a new variable

$$\eta \equiv xy^m. \tag{55}$$

The transformation relations are then

$$\frac{\partial}{\partial x} = \frac{\partial}{\partial \eta}\frac{\partial \eta}{\partial x} + \frac{\partial}{\partial y}\frac{\partial y}{\partial x} = y^m \frac{\partial}{\partial \eta}, \tag{56}$$

$$\frac{\partial}{\partial y} = \frac{\partial}{\partial \eta}\frac{\partial \eta}{\partial y} + \frac{\partial}{\partial y}\frac{\partial y}{\partial y} = m\frac{\eta}{y}\frac{\partial}{\partial \eta} + \frac{\partial}{\partial y}. \tag{57}$$

In order to have matching conditions specified in terms of η and y, the inviscid solutions for the outer region are expressed as

$$f_{\text{outer}} = F(y)\,x = F(y)\,\eta/y^m, \quad h_{\text{outer}} = H(y)\,x^s = H(y)\,\eta^s/y^{ms}. \tag{58), (59}$$

Concomitantly, the corresponding solutions for the inner region must be of the form

$$f_{\text{inner}} = f(\eta, y)/y^m, \quad h_{\text{inner}} = h(\eta, y)/y^{ms}. \tag{60), (61}$$

The matching conditions thus become

$$F(y)\,\eta = f(\eta, y) \quad \text{at some} \quad \eta = \tilde{\eta}, \tag{62}$$

$$H(y)\,\eta^s = h(\eta, y) \quad \text{at some} \quad \eta = \tilde{\eta}. \tag{63}$$

Equations (33)–(35) become

$$\lambda m \frac{\partial \ln h}{\partial \ln \eta} + \lambda \frac{\partial \ln h}{\partial \ln y} - \left(1 - \frac{f}{x}\right)\frac{\partial \ln h}{\partial \ln \eta} + \frac{f}{x}\left(\frac{\partial \ln f}{\partial \ln \eta} + j\right) = 0, \tag{64}$$

$$\frac{\partial \ln g}{\partial \ln \eta} = 0, \tag{65}$$

$$-\lambda + \lambda m \frac{\partial \ln g}{\partial \ln \eta} + \lambda \frac{\partial \ln g}{\partial \ln y} - \gamma\left[\lambda m \frac{\partial \ln h}{\partial \ln \eta} + \lambda \frac{\partial \ln h}{\partial \ln y} - \left(1 - \frac{f}{x}\right)\frac{\partial \ln h}{\partial \ln \eta}\right]$$

$$= A(y)\frac{g^\alpha}{h^{2+\alpha-\delta}}\left[\frac{\partial^2 h}{\partial \eta^2} + \frac{j}{\eta}\frac{\partial h}{\partial \eta} - \frac{(2+\alpha-\delta)}{h}\left(\frac{\partial h}{\partial \eta}\right)^2\right] y^{(2+\alpha-\delta)ms + m(2-s) + 0\cdot 5 - \alpha - (j+1)^{-1}}. \tag{66}$$

In the above,

$$A(y) = \frac{\gamma^{\alpha+1}}{RP}\frac{y^{(j+1)^{-1}}}{\xi} \tag{67}$$

and is finite for all y. The parameters f and h are functions of η and y, as specified by (62) and (63). For the right-hand side of (66) to be finite, the exponent of y must be zero. Thus

$$m = (\alpha - \alpha_s)/(s + \alpha s + 2 - \delta s). \tag{68}$$

9. Reduction to ordinary differential equations

To simplify the solution of the problem, co-ordinate expansions for the dependent variables are introduced. We write

$$f(\eta, y) = f_0(y) + f_1(y)\,\eta + f_2(y)\,\eta^2 + f_3(y)\,\eta^3, \tag{69}$$

and

$$h(\eta, y) = h_0(y) + h_1(y)\,\eta + h_2(y)\eta^2 + h_3(y)\,\eta^3. \tag{70}$$

The boundary conditions are

$$f = 0 \quad \text{at} \quad \eta = 0, \qquad \text{and} \qquad \partial h/\partial\eta = 0 \quad \text{at} \quad \eta = 0. \tag{71),(72}$$

In order to satisfy these, it follows from (64)–(66) that

$$f_0(y) = f_2(y) = h_1(y) = h_3(y) = 0. \tag{73}$$

Equations (69) and (70) then reduce to

$$f(\eta, y) = f_1(y)\,\eta + f_3(y)\,\eta^3 \quad \text{and} \quad h(\eta, y) = h_0(y) + h_2(y)\,\eta^2. \tag{69a),(70a)}$$

Substituting these expressions into (62)–(64) and (66), and equating like powers of η, we obtain the following set of ordinary differential equations for the determination of the five unknown functions $f_1(y), f_3(y)$, $h_0(y)$, $h_2(y)$ and $\tilde{\eta}(y)$:

$$\lambda y \frac{h_0'}{h_0} + f_1(j+1) - \lambda m s = 0, \tag{74}$$

$$\lambda y \left(h_2' - \frac{h_2 h_0'}{h_0}\right) - (1 - f_1 - \lambda m)\,2h_2 + (j+3) f_3 h_0 = 0, \tag{75}$$

$$-\lambda + \lambda y \frac{g'}{g} - \lambda\gamma y \frac{h_0'}{h_0} + \gamma\lambda m s = A(y)\,2(j+1)\frac{g^\alpha}{h_0^{2+\alpha-\delta}} h_2, \tag{76}$$

$$h_0 + h_2\tilde{\eta}^2 = H(y)\,\tilde{\eta}^s, \tag{77}$$

$$f_1\tilde{\eta} + f_3\tilde{\eta}^3 = F(y)\,\tilde{\eta}. \tag{78}$$

Primes denote differentiation with respect to y.

10. Solution

The set of nonlinear equations (74)–(78) specifies, in effect, an initial-value problem. One must obtain first a solution for $y = 0$, to provide initial conditions for $y > 0$. The former is, of course, self-similar, the flow field then being a function of only one independent variable, η. Under such circumstances, (74)–(78) are reduced to the algebraic relations

$$f_1(0) = ms, \tag{79}$$

$$-(1 - f_1(0) - \lambda_0 m)\,2h_2(0) + (j+3) f_3(0)\,h_0(0) = 0, \tag{80}$$

$$1 - \gamma m s = 2A(0)\frac{g(0)^\alpha}{h_0(0)^{2+\alpha-\delta}} h_2(0), \tag{81}$$

$$h_0(0) + h_2(0)\,\tilde{\eta}^2(0) = k_1\tilde{\eta}^s(0), \tag{82}$$

$$f_1(0) + f_3(0)\,\tilde{\eta}^2(0) = \gamma^{-1}. \tag{83}$$

Proper account has been taken of the fact that, for $y = 0$, $\lambda = \lambda_0 = j+1$. Equations (79)–(83) are solved directly, yielding

$$f_{\text{inner}} = (f_1(0)\,\tilde{\eta}(0) + f_3(0)\,\tilde{\eta}^3(0))/y^m = f_1^*(0)\,\tilde{\eta}(0) + f_3^*(0)\,\tilde{\eta}^3(0), \tag{84}$$

$$h_{\text{inner}} = (h_0(0) + h_2(0)\,\tilde{\eta}^2(0))/y^{ms} = h_0^*(0) + h_2^*(0)\,\tilde{\eta}^2(0), \tag{85}$$

$$\tilde{x}(0) = \tilde{\eta}(0)/y^m. \tag{86}$$

Although (84)–(86) indeed furnish the initial conditions for the case $y > 0$, the system of governing equations is singular at $y = 0$, so that one cannot start numerical integration at this point. To overcome this, following the established procedure, an expansion for small y is introduced. In particular, we postulate that, in the vicinity of $y = 0$, we can write

$$f_1(y) = f_1(0) + ly, \tag{87}$$

while

$$A(y) = p_1 + p_2 y. \tag{88}$$

Here, according to definition (67),

$$p_1 = \frac{\gamma^{\alpha+1}}{RP}\,(\xi_1^{(j+1)^{-1}})^{-1} \quad \text{and} \quad p_2 = -p_1(j+1)^{-1}\,\xi_2. \tag{89), (90}$$

Equations (74) and (76) then yield, respectively,

$$h_0(y) = h_0(0)\,\{1 - ny\} = h_0(0)\,\{1 - (l - (\lambda_1/\lambda_0)\,ms)\,y\}, \tag{91}$$

$$h_2(y) = h_2(0)\,(1 + by), \tag{92}$$

where

$$b = u_1 n + v_1, \tag{93}$$

with

$$u_1 = \frac{-\gamma}{1 - \gamma ms} - 2 - \alpha + \delta, \tag{94}$$

$$v_1 = \frac{\lambda_1}{\lambda_0} - \frac{p_2}{p_1} - \alpha\frac{g_1}{g_0} - \frac{g_1}{g_0}\frac{1}{(1-\gamma ms)}. \tag{95}$$

From (75), then,

$$f_3(y) = f_3(0)\,(1 + cy), \tag{96}$$

where

$$c = u_2 n + v_2, \tag{97}$$

with

$$u_2 = \frac{-1 - \frac{1}{2}\lambda_0}{1 - ms - m\lambda_0} + 1 + u_1 - \frac{\lambda_0}{2}\frac{u_1}{(1 - ms - m\lambda_0)}, \tag{98}$$

$$v_2 = \frac{-(\lambda_1/\lambda_0)\,ms - m\lambda_1}{1 - ms - m\lambda_0} + v_1 - \frac{\lambda_0}{2}v_1\frac{1}{1 - ms - m\lambda_0}. \tag{99}$$

Finally, the matching point, near $y = 0$, is found from (78) to be at

$$\tilde{\eta}(y) = \tilde{\eta}(0)\,(1 + dy), \tag{100}$$

where

$$d = u_3 n + v_3, \tag{101}$$

with

$$u_3 = \frac{1}{2}\left(-u_2 - \frac{\gamma}{1 - \gamma ms}\right), \tag{102}$$

$$v_3 = \frac{1}{2}\left\{v_2 + \left(\frac{\lambda_1}{\lambda_0} - \frac{g_1}{g_0} - \gamma\frac{\lambda_1}{\lambda_0}ms\right)(1 - \gamma ms)^{-1}\right\}. \tag{103}$$

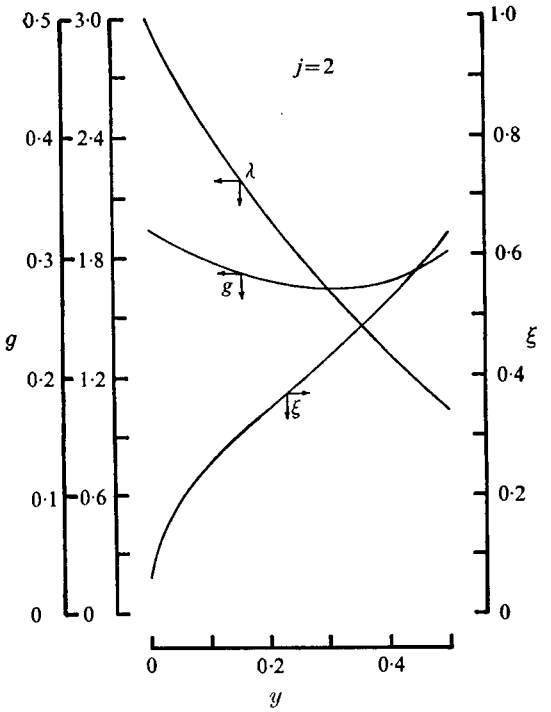

FIGURE 1. Decay parameter λ, non-dimensional pressure at the centre g, and the front co-ordinate ξ, as functions of the front intensity $y = M^{-2}$, for the outer inviscid region in the point-symmetrical case ($j = 2$).

Equations (87), (91), (92), (96) and (100) are now substituted into (77), to give (see (87) and (91))

$$n = \frac{[k_1\tilde{\eta}^s(0)\,(sv_3 - s\lambda_1/\lambda_0 + (\gamma-1)^{-1}g_1/g_0) - h_2(0)\,\tilde{\eta}^2(0)\,(v_1+2v_3)]}{[h_2(0)\,\tilde{\eta}^2(0)\,(u_1+2u_3) - k_1\tilde{\eta}^s(0)\,su_3 - h_0(0)]}. \quad (104)$$

The integration can be started on the basis of this result.

11. Results

The numerical results presented here serve only as illustrations of the type of data obtainable by the analytical technique we developed. They all refer to the classical case of point explosions with non-zero counter-pressure in a perfect gas with $\gamma = 1{\cdot}4$. The properties of the inviscid, outer regime of the blast wave are based on the data of Korobeinikov & Chushkin (1966), and displayed here in figures 1–3 for $j = 2$, 1 and 0, respectively. On this basis, the coefficients of the algebraic relations specifying the functions $\lambda(y)$, $g(y)$ and $\xi(y)$, (48)–(50), are given in tables 2–4. They provide accurate approximations to the numerical results of Korobeinikov & Chushkin (1966) in the range $0 \leqslant y < 0{\cdot}5$.

The reference radius of the front co-ordinate ξ is directly related to the explosion energy E_0 by

$$r_0 = b_0(E_0/p_a)^{(j+1)^{-1}}. \quad (105)$$

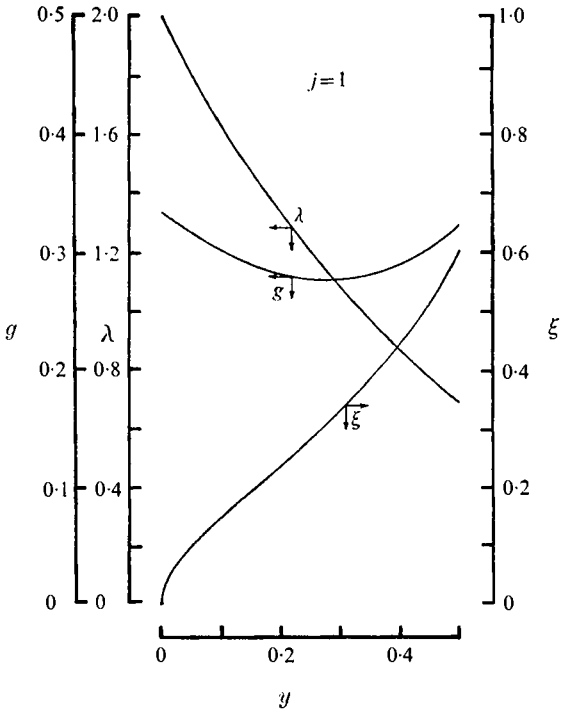

FIGURE 2. $\lambda(y)$, $g(y)$ and $\xi(y)$ for the outer inviscid region in the line-symmetrical case ($j = 1$).

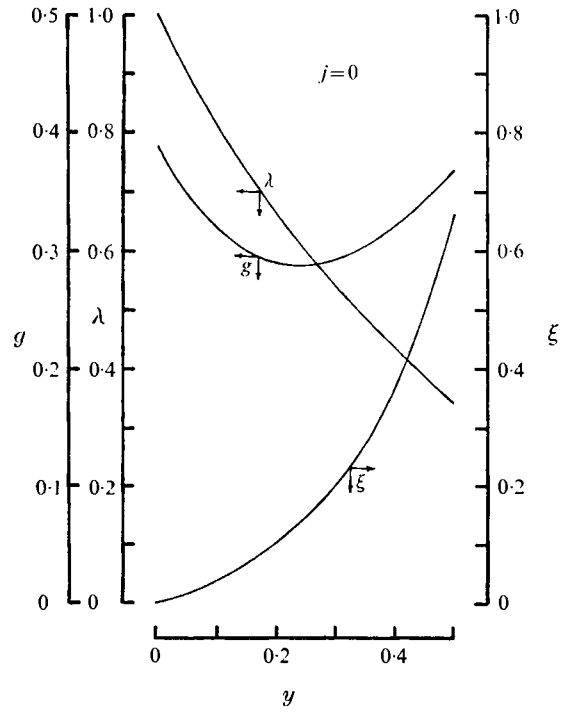

FIGURE 3. $\lambda(y)$, $g(y)$ and $\xi(y)$ for the outer inviscid region in the plane-symmetrical case ($j = 0$).

j	λ_0	λ_1	λ_2	λ_3	λ_4
0	1·0	−2·15	2·86	−3·12	1·45
1	2·0	−4·30	5·72	−6·24	2·90
2	3·0	−6·44	8·58	−9·35	4·35

TABLE 2. Coefficients in expansion of $\lambda(y)$ (equation (48))

j	g_0	g_1	g_2	g_3	g_4
0	0·389	−0·935	2·46	−1·54	0·362
1	0·333	−0·372	0·477	0·509	−0·146
2	0·323	−0·372	0·938	−0·134	1·58

TABLE 3. Coefficients in expansion of $g(y)$ (equation (49))

j	ξ_1	ξ_2	ξ_3	ξ_4	ξ_5	ξ_6	ξ_7	ξ_8	ξ_9
0	0·317	6·44	$-9·11^{1}$†	$1·93^{3}$	$-1·66^{4}$	$7·37^{4}$	$-1·79^{5}$	$2·26^{5}$	$-1·16^{5}$
1	0·179	6·44	3·32	$-8·18^{1}$	$6·62^{2}$	$-2·27^{3}$	$3·51^{3}$	$-2·00^{3}$	0
2	0·114	6·44	$5·41^{1}$	$-1·18^{3}$	$1·10^{4}$	$-5·24^{4}$	$1·36^{5}$	$-1·81^{5}$	$9·65^{4}$

† Shorthand notation for powers of ten is used, so e.g. $-9·11^{1} \equiv -9·11 \times 10^{1}$.

TABLE 4. Coefficients in expansion of $\xi(y)$ (equation (50))

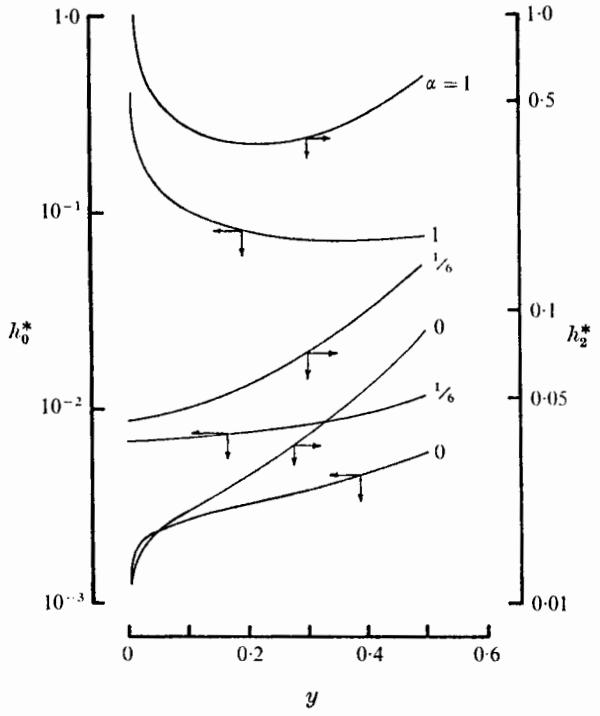

FIGURE 4. Integral curves of density coefficients $h_0^*(y)$ and $h_2^*(y)$ for $RP = 10^4, j = 2$ and various α.

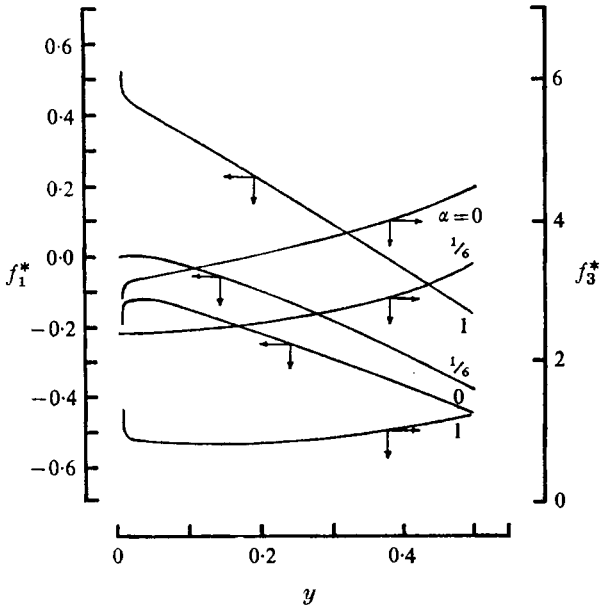

FIGURE 5. Integral curves of velocity coefficients $f_1^*(y)$ and $f_3^*(y)$ for $RP = 10^4, j = 2$ and various α.

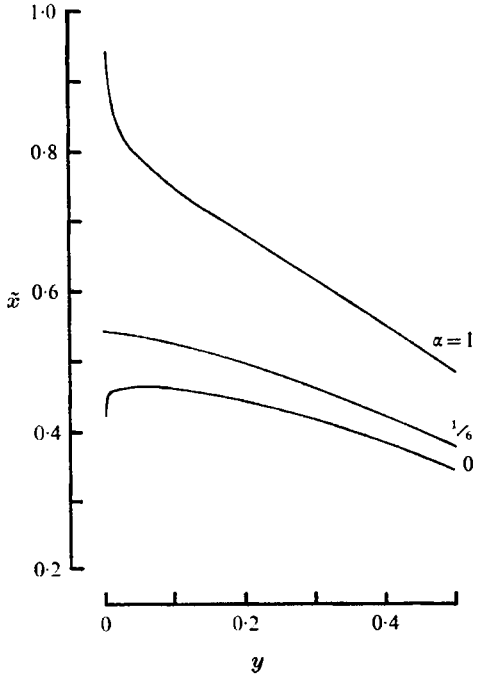

FIGURE 6. Location of matching point $\tilde{x}(y)$ for $RP = 10^4, j = 2$ and various α.

b_0 is a number close to unity (see e.g. Sedov 1959, p. 231). From the definition (16) of ϵ, and the Reynolds number (9), it follows that $\epsilon \propto r_0^{-1} \propto E_0^{-(j+1)^{-1}}$, so that the extent of the inner region is of order $\nu(\epsilon) = \epsilon^{\omega} \propto E_0^{-\omega/(j+1)}$. According to table 1, we have $\frac{1}{17} \leqslant \omega \leqslant 1/3{\cdot}25$ for the various values of j, δ and α listed, so the exponent $-\omega/(j+1)$ of E_0 lies in the range $-1/3{\cdot}25 \leqslant -\omega/(j+1) \leqslant -\frac{1}{51}$. The implication of E having this quite small negative exponent is that the size of the inner region is relatively insensitive to the energy of the explosion.

In order to explore the salient features of the results, they are first worked out for the case of the Reynolds–Prandtl number product $RP = 10^4$, and three typical values of the temperature exponent, α, for the viscosity coefficient, while radiation effects have been neglected ($\delta = 0$). These solutions serve also as a demonstration that thermal conduction as the sole heat-transfer mechanism is generally insufficient to lower the temperatures near the centre to a level compatible with the assumption that radiation is negligible. The results are specified in terms of integral curves for $h_0^*(y)$, $h_2^*(y)$, $f_1^*(y)$, $f_3^*(y)$ and $\tilde{x}(y)$, displayed in figure 4–6 for the case of $j = 2$. We note that, for this value of j, one has a saddle-point singularity at $y = 0$. Its axes are provided by the ordinate $y = 0$ and the integral curve for $\alpha = \alpha_s$ having the value of $\frac{1}{6}$. Although the results for $j = 1$ and $j = 0$ are not plotted, they show the same behaviour, with the axes passing through the saddle point given by $y = 0$ and the integral curves for $\alpha = \alpha_s$ with the values 0 and $-\frac{1}{2}$, respectively.

Temperature profiles for this non-radiative case are shown in figure 7† for $j = 2$ and the same values of α as in figures 4–6. (The temperature is non-dimensionalized by T_n, the value behind the shock wave.) We see from the figure that for $\alpha = \frac{1}{6}$ and $\alpha = 0$ the temperatures in the inner region vary from about 20 to over 500 times the temperature at the shock. Since for the lowest Mach number shown, $M = \sqrt{2}$, corresponding to $y = 0{\cdot}5$, $T_n = O$ (360 °K), temperatures in the inner region for these cases will lie between 7200 and 180 000 °K, with the average temperatures so high that the effects of radiation are predominant. For the case of $\alpha = 1$, on the other hand, we see that the temperatures are sufficiently low (of the order of 3600 °K), so that conduction will be the dominant heat-transfer mechanism. The temperature profiles for the $j = 0$ and $j = 1$ cases are shown in figures 8 and 9. Neglect of radiation is possible only for $\alpha = 1$ when $j = 1$ and for $\alpha = 1$ or 0 when $j = 0$: for each j, it becomes less valid as α decreases, reflecting the fact that the smaller α is, the less effective is thermal conduction in reducing the high temperatures near the centre. In figures 10–12 are shown the location of the matching point, and non-dimensional density and velocity profiles for some of the cases just described, for which heat conduction alone is a valid model.

† In figure 7 and all later figures that exhibit x profiles, the curves do not extend up to $x = 1$, which is the location of the shock at that time, because the approximate expressions (48)–(50), introduced to represent analytically the outer inviscid regions, are most accurate in the vicinity of matching of the inner and outer regions, and are not good approximations further out. The parts of the curves thus omitted can be obtained from the inviscid solutions of Korobeinikov & Chushkin (1966). In addition, since, to emphasize the distinctions between the inner and outer regions, we have not developed composite expansions, this and the following figures show profiles that are not smooth at the points where the inner and outer solutions join.

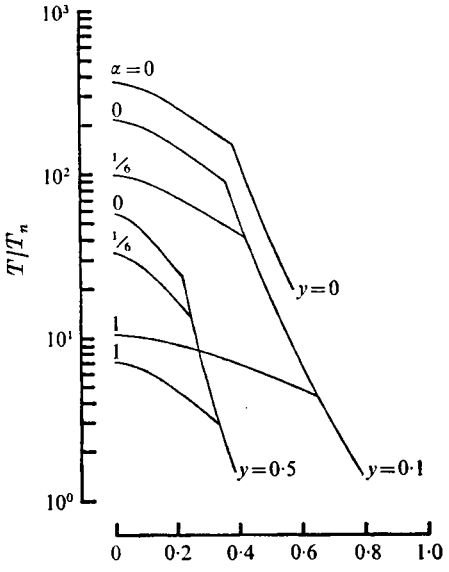

FIGURE 7

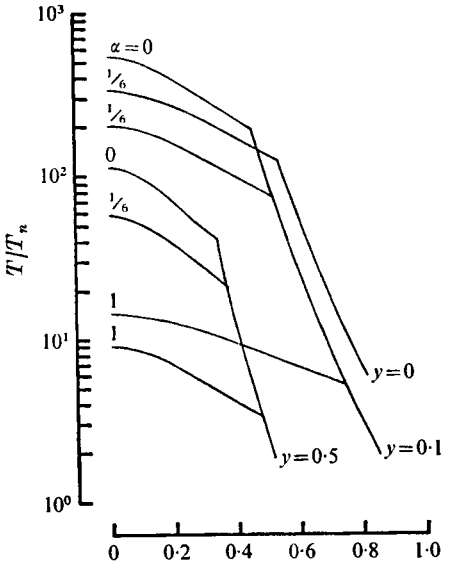

FIGURE 8

FIGURE 7. Temperature profiles for $RP = 10^4, j = 2$ and various values of the temperature exponent α and front velocity parameter y.

FIGURE 8. Temperature profiles for $RP = 10^4, j = 1$ and various values of the temperature exponent α and front velocity parameter y.

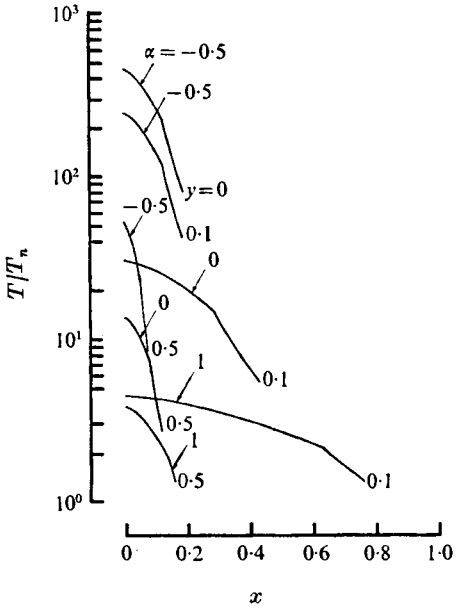

FIGURE 9. Temperature profiles for $RP = 10^4, j = 0$ and various values of the temperature exponent α and front velocity parameter y.

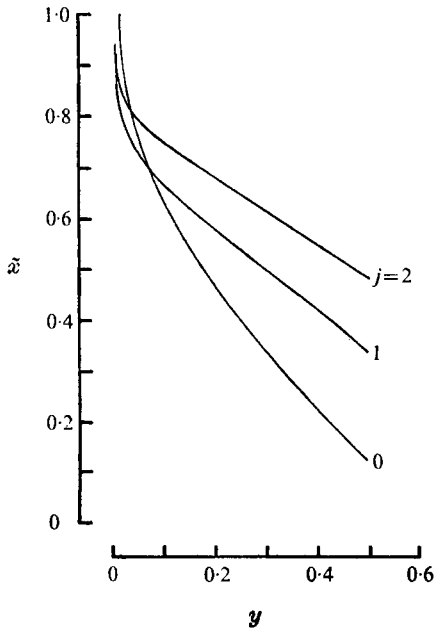

FIGURE 10. Location of matching point $\tilde{x}(y)$ for $RP = 10^4$, $\alpha = 1$ and $j = 0, 1, 2$.

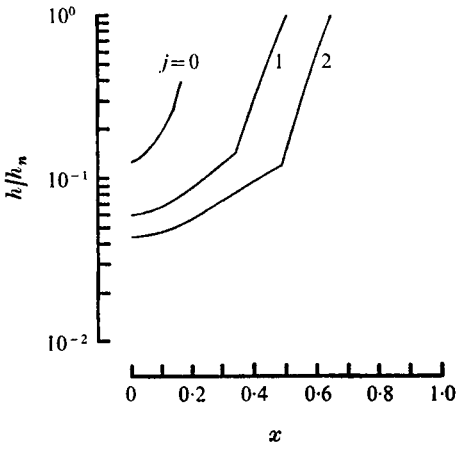

FIGURE 11. Density profiles for $RP = 10^4$, $\alpha = 1$, $y = 0{\cdot}5$ and $j = 0, 1, 2$.

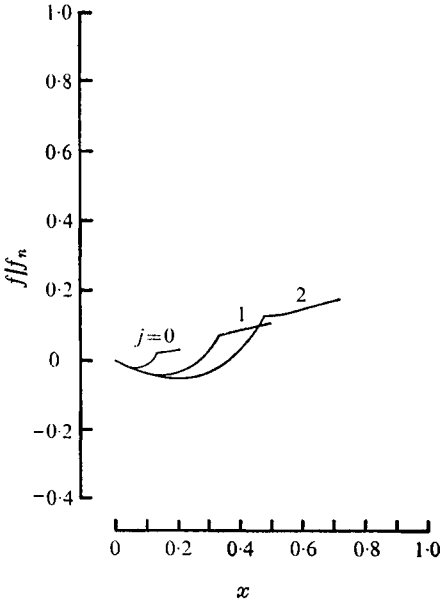

FIGURE 12. Velocity profiles for $RP = 10^4$, $\alpha = 1$, $y = 0{\cdot}5$ and $j = 0, 1, 2$.

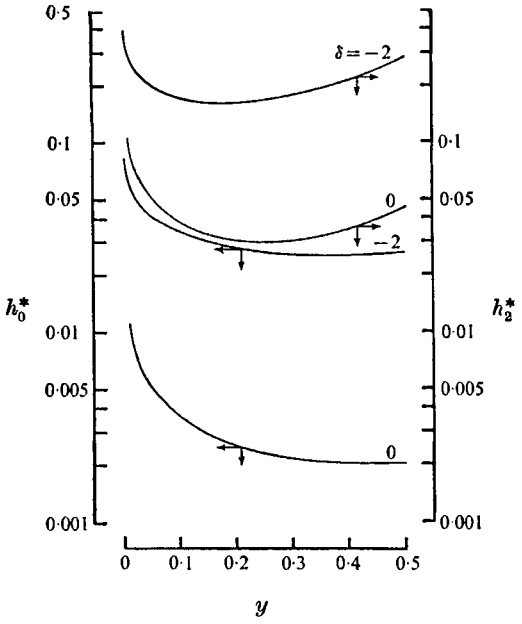

FIGURE 13. Integral curves of density coefficients $h_0^*(y)$ and $h_2^*(y)$ for $RP = 10^9$, $j = 2$, $\alpha = 1{\cdot}5$ and $\delta = 0$ and -2.

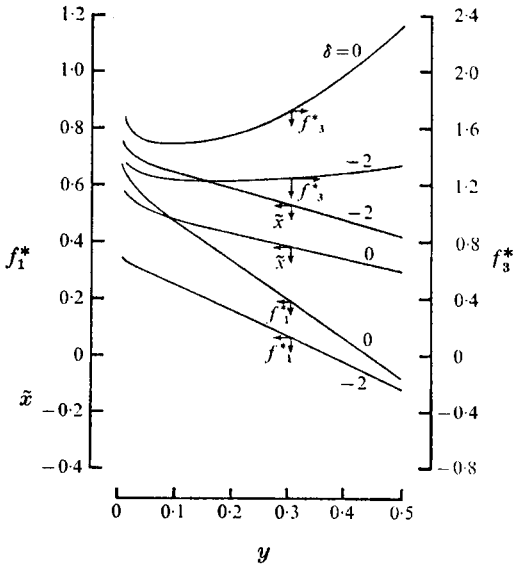

FIGURE 14. Integral curves of velocity coefficients $f_1^*(y)$ and $f_3^*(y)$, and location of matching point $\tilde{x}(y)$ for $RP = 10^9$, $j = 2$, $\alpha = 1{\cdot}5$ and $\delta = 0$ and -2.

To investigate the effects of radiation, integral curves have also been obtained for the physically most interesting case, the point explosion ($j = 2$), with $RP = 10^9$ (corresponding to an explosion energy $E_0 = 10^{23}$ ergs, equivalent to a yield of about 100 times that of the first nuclear bomb test at Alamogordo). The proper values of the parameters α and δ appearing in (8) can be obtained from the data for the properties of high-temperature air for the pertinent temperature–density range of interest. From the data of Armstrong *et al.* (1961) (see also Scala & Sampson 1964), curve-fitting their values for the Rosseland mean free path, we find that appropriate values for the cases we calculate are $\alpha = 1{\cdot}5$ and $\delta = -2$. Integral curves of the density and velocity coefficients and location of the matching point between inner and outer expansions are shown in figures 13 and 14. In addition to the radiation case of $\delta = -2$, for comparison purposes we also show in these figures, and the ones that follow, corresponding curves for the non-radiation case $\delta = 0$. The density, velocity and temperature profiles calculated from these coefficients are shown in figures 15–17. The inclusion of radiation is seen to have the effect of flattening the density and temperature profiles. (It is worthy of note that, because the pressure is nearly constant in the inner region, a decrease in the value of δ is equivalent to an increase in α. Thus the flattening of profiles, just described, which occurs as we go from the non-radiative $\delta = 0$ case to the radiative $\delta = -2$ case, occurs in each of the purely non-radiative cases as α increases from 0 or $-\frac{1}{2}$ to the value 1.) Furthermore, temperatures in the inner region are decreased, and densities correspondingly increased, by about one order of magnitude, with radiation taken into account.

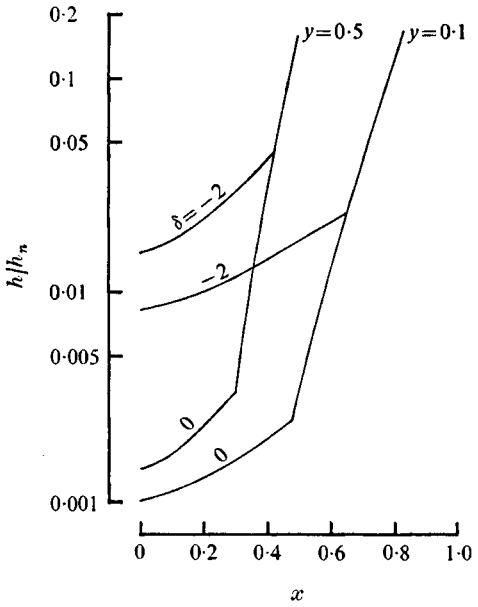

FIGURE 15. Density profiles for $RP = 10^9$, $j = 2$, $\alpha = 1{\cdot}5$, $\delta = 0$ and -2, and various values of front velocity parameter y.

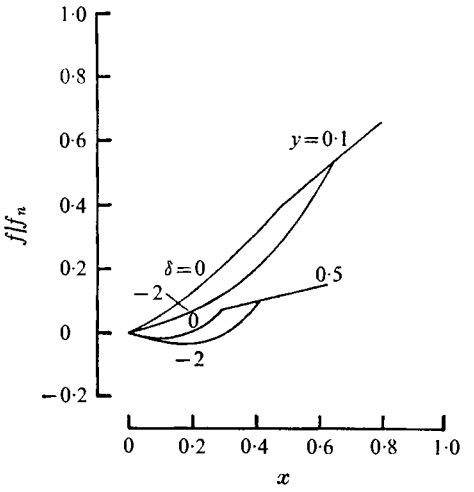

FIGURE 16. Velocity profiles for $RP = 10^9$, $j = 2$, $\alpha = 1{\cdot}5$, $\delta = 0$ and -2, and various values of the front velocity parameter y.

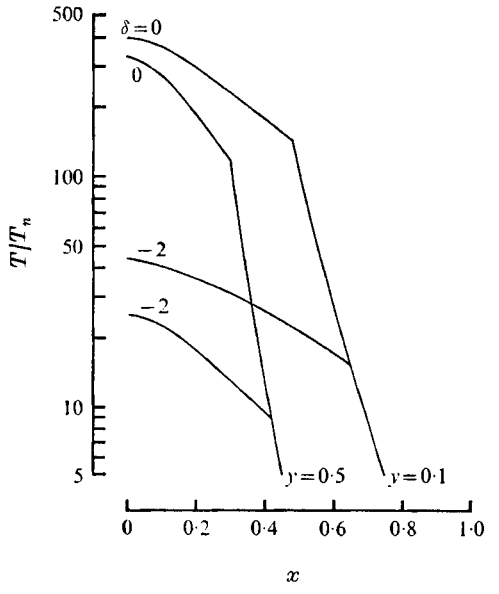

FIGURE 17. Temperature profiles for $RP = 10^9$, $j = 2$, $\alpha = 1{\cdot}5$, $\delta = 0$ and -2, and various values of the front velocity parameter y.

The density and temperature profiles for this high-energy explosion ($RP = 10^9$) and the extent of the inner region agree qualitatively with the comprehensive fully-numerical calculations of Brode (1968) for nuclear explosions, especially at times when the present solution might be expected to be valid. That is, Brode's calculations show, as do the results here, a steep increase in temperature as one moves inwards from the shock, until a point about 40–60 % of the distance to the shock is reached. After this the temperature remains relatively uniform and high, up to the centre. That there is only a mild temperature gradient in the inner region is a consequence of the highly nonlinear dependence of the thermal conductivity χ on temperature when the Rosseland approximation for radiation is made. For the effect of this nonlinear dependence on the energy equation is such that the heat in the central region cannot instantaneously penetrate over large distances, but propagates with a finite velocity, in such a way that a sharply defined boundary exists between the hot region and the colder region not yet reached by the thermal disturbance (Zel'dovich & Raizer 1967, ch. 10). Thus the heat propagates in the form of a wave, which is actually referred to as a *thermal wave* or, alternatively, *radiation front*. Immediately upon the initiation of a blast of extremely high energy, the speed of propagation of the thermal wave is much greater than the speed of sound. (In fact, for the spherical case, the speed of the wave $dr_f/dt \sim T^{n+\frac{1}{2}}$, where n is the exponent in the expression $\chi \sim T^n$. Since the pressure is constant in the inner region, $\chi \sim T^{3\cdot5}$ for our choice $\alpha = 1\cdot5, \delta = -2$, and consequently $dr_f/dt \sim T^{3\cdot83}$, whereas the speed of sound in a high-temperature gas is roughly proportional to $T^{\frac{1}{2}}$.) Thus, initially there is little motion of the fluid, and the heat flows through a stationary medium as a thermal wave. As the temperature falls, this wave decelerates while the fluid is set in motion. This leads to the formation of a shock wave, which eventually overtakes the thermal wave. It is at this later stage, at a time of the order perhaps of a millisecond after initiation, that the blast begins to resemble the classical strong-explosion solution. Our results are valid only for times subsequent to this initial period of transition from radiative to shock growth.

This work was supported by the U.S. Air Force Office of Scientific Research, under grant AFOSR 72-2200; by N.A.S.A., under grant NSG-702/05-003-050; and by the National Science Foundation, under grant GK-229754A1.

REFERENCES

ARMSTRONG, B. H., SOKOLOFF, J., NICHOLLS, R. W., HOLLAND, D. H. & MEYEROTT, R. E. 1961 Radiative properties of high-temperature air. *J. Quant. Spectroscopy Rad. Trans.* **1**, 143.

BACH, G. G., KNYSTAUTAS, R. & LEE, J. H. S. 1969 Direct initiation of spherical detonations in gaseous explosions. *Proc. 12th Int. Symp. Combust.*, p. 853.

BACH, G. G. & LEE, J. H. S. 1970 An analytical solution for blast waves. *A.I.A.A. J.* **8**, 271.

BOWEN, J. R. & FEAY, B. A. 1970 A refinement of the cylindrical blast wave. *Astronautica Acta*, **15**, 275.

BRODE, H. L. 1955 Numerical solutions of spherical blast waves. *J. Appl. Phys.* **26**, 766.

BRODE, H. L. 1968 Review of nuclear weapons effects. *Annual Review of Nuclear Science*, **18**, 153.

BRUECKNER, K. A. 1973 Laser-driven fusion. *Abstracts 4th Int. Colloquium on Gas Dynamics of Explosions and Reactive Systems.*

GOULARD, R. 1964 Radiation transfer regimes in hypersonic flight. *Supersonic Flow, Chemical Processes and Radiative Transfer* (ed. D. B. Olfe & V. Zakkay). Pergamon.

KAMEL, M. M. & OPPENHEIM, A. K. 1971 Laser cinematography of explosions. *Int. Center for Mechanical Sciences.*

KOROBEINIKOV, V. P. 1957 On the propagation of strong spherical blast waves in heat conducting gases. *Dokl. Acad. Nauk SSSR*, **113**, 1006.

KOROBEINIKOV, V. P. & CHUSHKIN, P. I. 1966 Plane, cylindrical and spherical blast waves in a gas with counter pressure. *Proc. V. A. Steklov Inst. Math.*

LEE, J. H., SOLOUKHIN, R. I. & OPPENHEIM, A. K. 1969 Current views on gaseous detonation. *Astronautica Acta*, **14**, 565.

OPPENHEIM, A. K., LUNDSTROM, E. A., KUHL, A. L. & KAMEL, M. M. 1971 A systematic exposition of the conservation equations for blast waves. *J. Appl. Mech.* **38**, 783.

OPPENHEIM, A. K. & SOLOUKHIN, R. I. 1973 Experiments in gasdynamics of explosions. *Ann. Rev. Fluid Mech.* **5**, 31.

PENNER, S. S. & OLFE, D. B. 1968 *Radiation and Re-entry.* Academic.

SCALA, S. M. & SAMPSON, D. H. 1964 Heat transfer in hypersonic flow with radiation and chemical reaction. *Supersonic Flow, Chemical Processes and Radiative Transfer* (ed. D. B. Olfe & V. Zakkay). Pergamon.

SEDOV, L. I. 1959 *Similarity and Dimensional Methods in Mechanics* (ed. M. Holt). Academic.

SYCHEV, V. V. 1965 On the theory of a strong explosion in heat-conducting gas. *Prikl. Mat. Mech.* **29**, 997.

THOMAS, M. & PENNER, S. S. 1964 Thermal conduction and radiant energy transfer in stationary, heated air. *Int. J. Heat Mass Transfer*, **7**, 1117.

VAN DYKE, M. 1964 *Perturbation Methods in Fluid Mechanics.* Academic.

VINCENTI, W. G. & KRUGER, C. H. 1965 *Introduction to Physical Gas Dynamics.* Wiley.

ZEL'DOVICH, YA. B. & RAIZER, YU. P. 1967 *Physics of Shock Waves and High-Temperature Hydrodynamic Phenomena* (ed. W. D. Hayes & R. F. Probstein), vol. 2. Academic.